

Performance evaluation of time-weighted backvalues least squares vs. NOGA track estimators via sensor data fusion and track fusion for small target detection applications

Neena Imam, Jacob Barhen, and Charles W. Glover
Center for Engineering Science Advanced Research, Computer Science and Mathematics
Division, Oak Ridge National Laboratory, Oak Ridge, Tennessee 37831

ABSTRACT

The rapid growth and increasing sophistication of airborne surveillance technology have spurred intense research efforts in the development and implementation of tracking algorithms capable of processing a large number of targets using multi-sensor data. In this paper, a novel tracking algorithm, the NOGA tracker, is presented and compared with the more conventional Time-Weighted Backvalues Least Squares (TWBLS) estimator for accuracy (numerical and phenomenological), ease of implementation, and time performance. The NOGA tracker combines model predictions and sensor measurements to produce best estimates for quantities of interest. The state estimator model used for NOGA is a simple second order auto-regression which is combined with an uncertainty reduction scheme involving nonlinear Lagrange optimization process in which the inverse of a global covariance matrix is used as the natural metric for the Bayesian inference that underlies the combining process. The NOGA tracker explicitly incorporates sensor and model uncertainties in the estimation process, and uses model sensitivities to propagate the associated covariance matrices accurately and in a systematic way.

Keywords: Uncertainty reduction, track fusion, sensor fusion, multi-sensor tracking, auto-regressive.

This work was supported by the Missile Defense Agency of the Department of Defense (NI and JB) and partially by the Materials Science and Engineering Division of the Department of Energy (JB) under contract number DE-AC05-00OR22725 with UT Battelle

1. INTRODUCTION

Missile defense test and evaluation platforms present very demanding technical requirements for precise visible and infrared signature data collection along with associated tracking in a densely cluttered multi-sensor multi-target environment. The Kalman filter/extended Kalman filter trackers, though optimal in the linear minimum mean square error (LMMSE) sense,¹ may not perform well for missile tracking applications since the targets are usually maneuvering. It also may not be possible to formulate the state and measurement vector equations in the form for Kalman filter implementation if the approximate forms of the target trajectories are not known. These facts motivated the authors of this paper to explore a multi-sensor multi-target algorithm based on time-weighted least squares back projection. Linear least squares algorithms have been applied successfully to problems in defense and missile flight analysis where rapid track hand over to the interceptor is mandatory.² Although based on previously published works, the Time-Weighted Back-values Least Squares (TWBLS) algorithm developed and discussed in this paper is original in its treatment of uncertainty calculation, incorporation of sensor data fusion, and track fusion schemes. A novel tracking algorithm, the NOGA tracker, is presented in parallel to the TWBLS algorithm. The state estimator model used for NOGA is a simple second order auto-regression which is combined with an uncertainty reduction scheme involving a fast, nonlinear Lagrange optimization process in which the inverse of a global covariance matrix is used as the natural metric for the Bayesian inference that underlies the combining process.³ The NOGA tracker explicitly incorporates sensor and model uncertainties in the estimation process and uses model sensitivities to propagate the associated covariance matrices accurately and in a systematic way. The next section outlines the system architecture assumed in this paper, along with sensor models. Section 3 presents the TWBLS algorithm including mathematical formulation, underlying mathematical assumptions, sensor data fusion, and track fusion implementation. Section 4 presents the NOGA tracker followed by description of ORNL developed uncertainty reduction method. The accuracy and time performance of the two algorithms are compared with the aid of numerical results. The paper concludes by outlining directions for future work with respect to improved algorithm accuracy and time performance. The issues of multi-target multi-sensor tracking in a cluttered environment and object-to-track association optimization are also addressed.

2. SYSTEM ARCHITECTURE

Modern missile defense sensors and interceptors employ the latest staring focal plane technology. For these highly demanding applications, it is customary to utilize multi-sensor platforms. Airborne surveillance platforms may employ dissimilar sensor groups for diverse sensor tasking. The system architecture considered in this paper mimics such a prototype airborne platform consisting of six staring sensors that are further differentiated into two separate groups. The three acquisition category sensors are less precise with larger integrated fields of view (*IFOV*) to provide broad area coverage of the surveillance region. The three tracking sensors have smaller *IFOV* and are suitable for more accurate target tracking. Three different sensor architectures are considered in this paper. First, a baseline single-target-single-sensor benchmark architecture is examined, where random observations derived from an analytical model are reported with an expectation rate of 33 Hz. Target azimuth and elevation estimates as functions of time are computed for both TWBLS and NOGA. The second architecture is a common multi-sensor architecture implemented in many airborne surveillance systems. The sensors are asynchronous and provide data to the estimators in a random order as show in Fig. 1A. Sensor data fusion is performed by a weighting factor (either linear or exponential) that grants more weight to most recent data and data from the more accurate tracking sensors with smaller *IFOV*. This preferential treatment of data facilitates estimation accuracy even though measurement data are accepted indiscriminately from sensors reporting in random order with varying degrees of measurement accuracy. The third architecture is more advanced and incorporates a track fusion node where the trackfiles received from synchronous acquisition and tracking sub-groups are fused in one global trackfile as shown in Fig. 1B. The track fusion technique is based on the weighted covariance fusion model.^{4, 5} The estimation uncertainties associated with the individual trackfiles may be further reduced after fusion hence providing

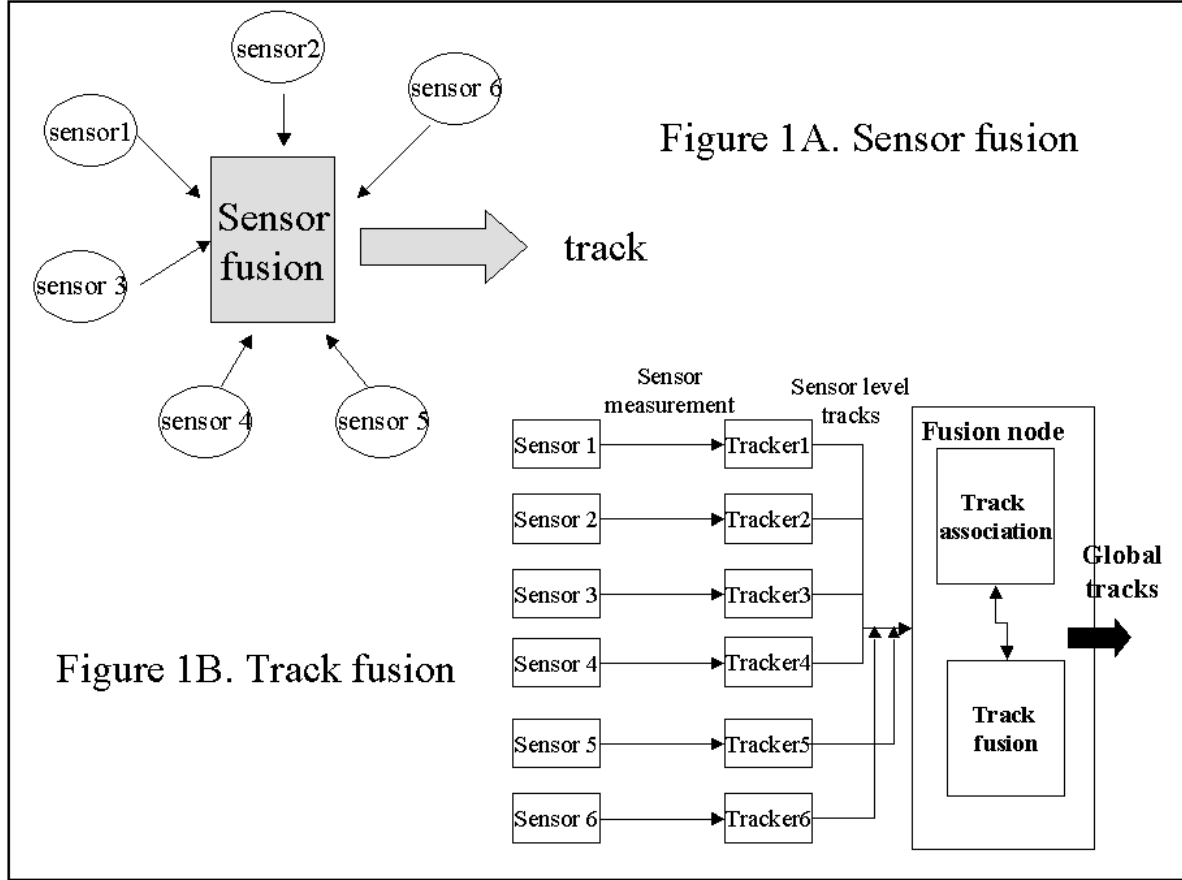


Figure 1: Multi-sensor fusion and track fusion architectures consisting of six asynchronous sensors (A) and six synchronous sensors and a fusion node implementing state vector fusion (B).

improved tracking accuracy. The use of multiple sensors for target tracking can potentially provide better performance than a single sensor due to better visibility and complementary information. Theoretically the best tracking performance is achieved by fusing the measurements from the sensors directly.⁶ However, due to communication or organizational constraints, many real-world systems have a hierarchical structure where the fusion system has no direct access to the sensor data. The sensor data are processed only locally to form sensor tracks. Track fusion is then needed to associate the sensor tracks and generate an improved target state estimate. As shown in Fig. 1B, single sensor track processors estimate single sensor tracks based on the TWBLS algorithm. Tracks from different sensors are periodically (on demand) sent to a central site to be fused. Track fusion involves two steps: association and target state estimation fusion. During association, tracks from different sensors are correlated to test for the hypothesis that the tracks all correspond to a single target. Given a correct association, the state estimates of the global track are obtained by fusing the state estimates of associated sensor tracks. For simplicity, it is assumed that the six local nodes generate tracks that relate to the same target and are derived in the same coordinate system. It is further assumed that the system is observable. The problem of time alignment and track association are not considered in the present work.

Sensor model and pseudo-random time sequence generation: For benchmark simulation purposes

a bounded random sighting sequence is generated with $t_0 = 0$, $t_N = t_{N-1} + \delta t_N$, where $\delta t_N = \delta_{min} + [\rho\delta_{max}/\delta_{min}]\delta_{min}$. Here ρ is a uniform number in $[0, 1]$, and δ_{max} represents the maximum delay of a new sighting beyond the minimum time increment δ_{min} . In many surveillance platforms the nominal sighting frequency is 30 Hz. This frequency can readily be achieved by proper selection of δ_{min} and δ_{max} .

For each sighting at t_N , the sensor provides the following quantities: r_n (target position such as azimuth and elevation) and Δr_N which is the standard deviation for sensor measurement. For the benchmark NOGA simulation, initial sensor uncertainties are constructed assuming constant relative error $\Delta r_N = \eta r_n$, where $\eta = 0.04$. For the TWBLS simulations, the sensor noise is assumed to be zero mean white Gaussian with standard deviation of 8% – 15%.

3. TIME-WEIGHTED BACKVALUES LEAST SQUARES ESTIMATOR (TWBLS)

The TWBLS algorithm can be extended to a multi-target multi-sensor framework although only a single target architecture is presented in this paper. The algorithm performs frame-to-frame target correlation using data from all six sensors to compile track histories with each track representing unique target. The least squares kernel accepts a list of sequential sensor measurements and generates tracks containing position and velocity as functions of time. The choice of coordinate frame is not relevant to the focus of this paper. It is assumed that the tracker estimates position as azimuth and elevation. However, the discussion presented in this paper can be readily extended to any reference frame of choice. The tracks store the temporal history of targets. It is assumed that all the local nodes generate tracks that relate to the same target and are derived in the same coordinate system. Issues such as track-to-track correlation, track initiation, and track maintenance are not discussed in this work but will be reported in a future paper.

3.1. Theoretical formulation

Least-squares back projection: The goal of the weighted least squares projection algorithm is to estimate the appropriate mathematical model to describe the functional relationship between variables x and y . Given a set of independent variables, x_1, x_2, \dots, x_N , and a set of dependent variables y_1, y_2, \dots, y_N , the coefficients a_1, a_2, \dots, a_M have to be determined such that

$$y_i = a_1 f_1(x_i) + a_2 f_2(x_i) + \dots + a_M f_M(x_i). \quad (1)$$

In order to employ matrix representation, vectors Y and C are defined as $Y = [y_1, y_2, \dots, y_N]^T$ and $C = [C_1, C_2, \dots, C_M]^T$, where Y is the N dimensional vector of dependent variables and C is the M dimensional vector of fitting coefficients. The functional matrix F has dimensions $N \times M$ and is represented as

$$F = \begin{pmatrix} f_1(x_1) & \dots & f_M(x_1) \\ \dots & \dots & \dots \\ f_1(x_N) & \dots & f_M(x_N) \end{pmatrix}_{N \times M}. \quad (2)$$

Equation 1 can be written as $Y_N = F_{NM} C_M$ or $F_{MN}^T Y_N = F_{MN}^T F_{NM} C_M$. A weight matrix can be included for preferential treatment of data to yield $F_{MN}^T W_{NN} Y_N = F_{MN}^T W_{NN} F_{NM} C_M$. If W is positive definite and $N \geq M$ then $F^T W F$ can be inverted to produce the well known “pseudo-inverse” solution for the vector of fitting coefficients

$$C_M = \left(F_{MN}^T W_{NN} F_{NM} \right)^{-1} F_{MN}^T W_{NN} Y_N. \quad (3)$$

Time and sensor data weighted least-squares back projection: The gate size or association region of the state estimator is the area within which the next target position is expected to fall. The gate size of the predicted target position at time t_N is precalculated at time t_{N-1} in order to associate the incoming detection

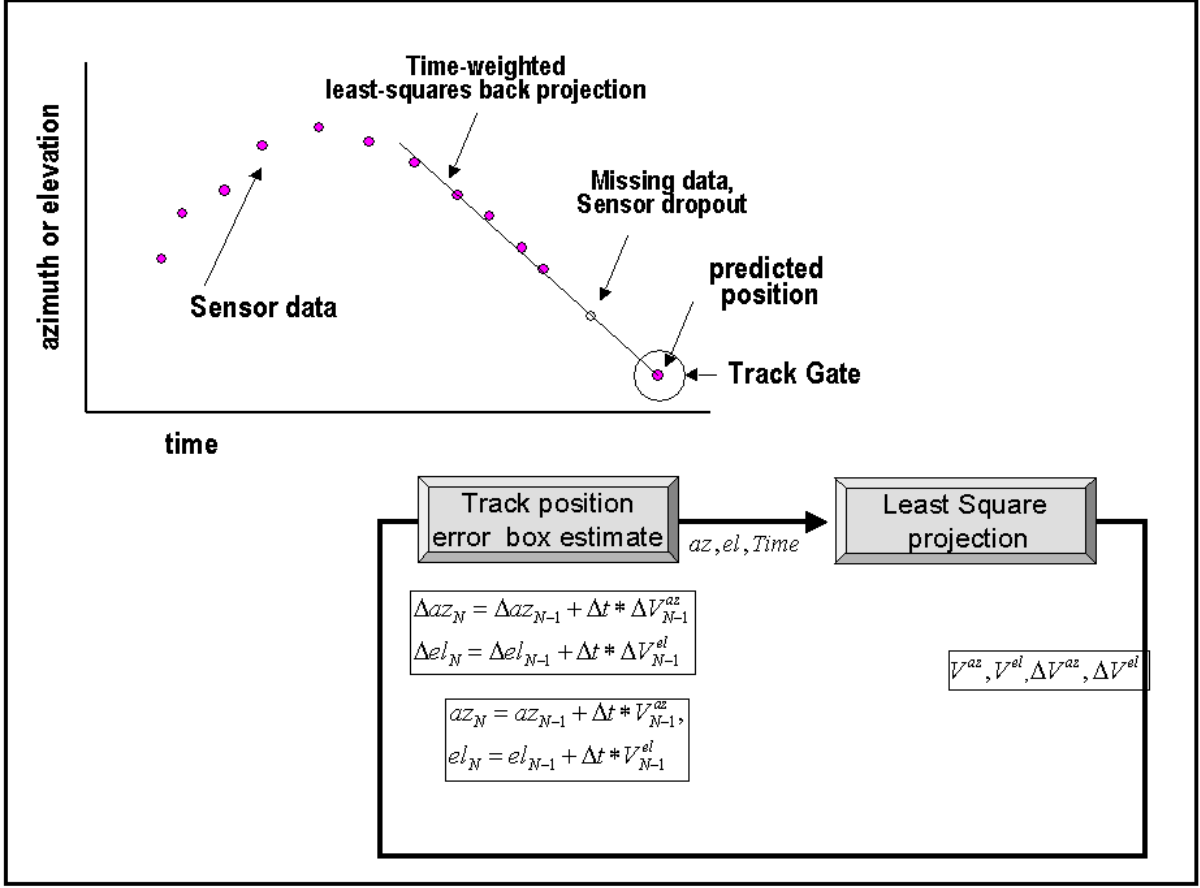


Figure 2: Straight line fit to the sensor position measurements to obtain velocity and ΔV .

(at time t_N) with any particular track. The gate size is calculated by using rates of change of azimuth and elevation (velocity $V^{az, el}$) and the uncertainties in the estimates of $\Delta V^{az, el}$. The velocities and associated uncertainties are calculated using a least squares projection based on N backvalues of sensor measurements. An object-to-track association process follows this step. To obtain velocity $V^{az, el}$ and $\Delta V^{az, el}$, azimuth and elevation values are fitted as linear functions of time. A straight line is fitted at each sensor measurement point. The slope of the straight line is the rate of change of azimuth/elevation and the error associated with the straight line fit is $\Delta V^{az, el}$, as shown in Fig. 2. The track velocity estimates are updated using a weighted linear least squares fit. Observations recorded during the last 600 msec ($N = 20$) are used. The weighting can be linear or exponential, with current observations and observations from the tracking sensors receiving maximum weight. The least squares fit produces estimates of the target velocity components as

$$az_N = \underbrace{C_1}_{V^{az}} \Delta t_N + C_2, \quad (4)$$

where $\Delta t_N = t_N - t_{N-1}$. Position uncertainties Δaz_N are computed using the velocity uncertainty times the propagation time from the last target observation to the current time. Tracks are propagated from their last observed position, using their last estimated velocity, to their predicted position at time t_N as

$$az_N = az_{N-1} + \Delta t \times V_{N-1}^{az}, \quad el_N = el_{N-1} + \Delta t \times V_{N-1}^{el}, \quad \Delta az_N = \Delta az_{N-1} + \Delta t \times \Delta V_{N-1}^{az} \quad (5)$$

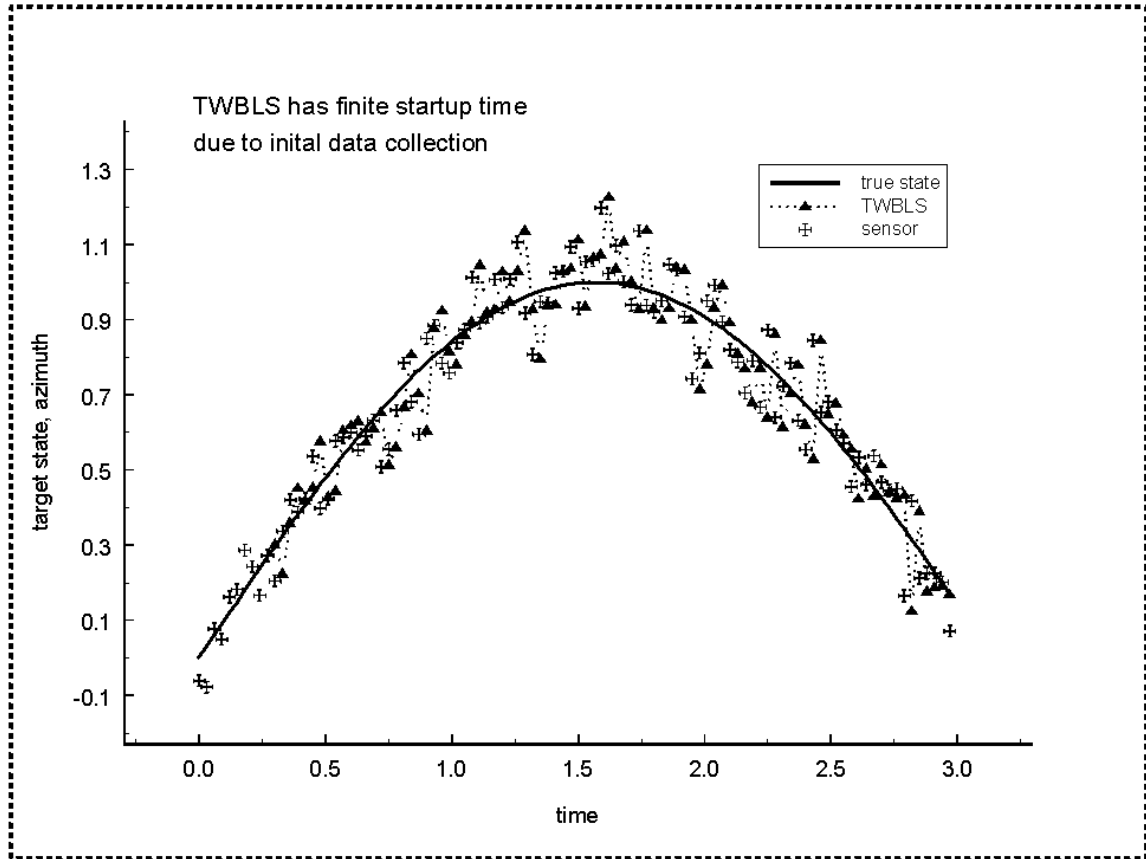


Figure 3: The state prediction of the TWBLS tracker.

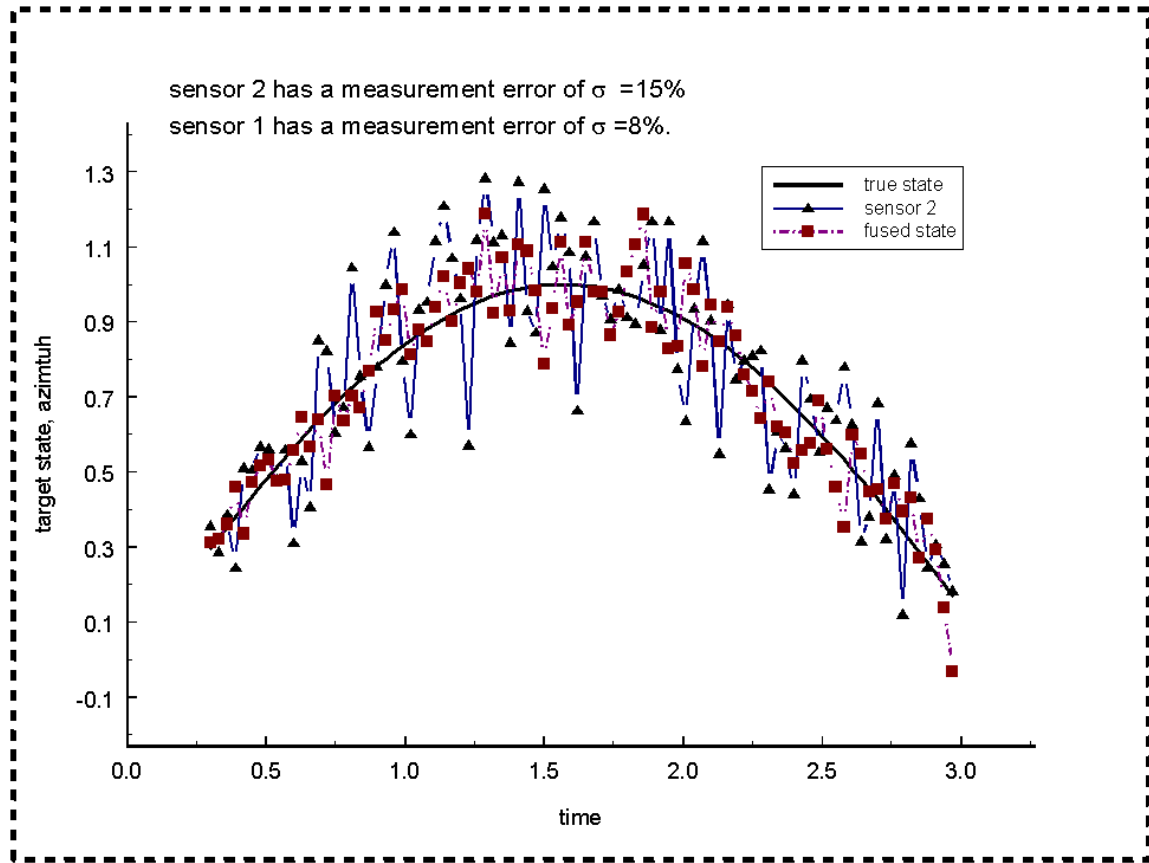
The center of the track gate is (az_N, el_N) and the gate extends according to 3σ where $\sigma = \Delta az_N$. Figure 3 shows the TWBLS state prediction along with the true target azimuth (for simplicity the target azimuth is modeled as $\sin(t)$) for a sensor noise standard deviation of 8%.

Sensor fusion: A nonlinear weight function $W = \exp^{-\Delta t / (IFOV)^2}$ is used to grant preferential treatment to data. The time matrix of backvalues is formulated as

$$F = \begin{pmatrix} \Delta t_N \frac{\exp^{-\Delta t_N}}{(IFOV)^2} & \frac{\exp^{-\Delta t_N}}{(IFOV)^2} \\ \vdots & \vdots \\ \Delta t_1 \frac{\exp^{-\Delta t_1}}{(IFOV)^2} & \frac{\exp^{-\Delta t_1}}{(IFOV)^2} \end{pmatrix}_{NX2} \quad (6)$$

The coefficient vector contains azimuth and elevation rates of change of informations as $C = [C_1 \ C_2]^T$. Least squares “pseudo-inverse” solution is used to solve for V and ΔV as $C_{az} = (F^T F)^{-1} F^T Y_{az}$. Since Δt increases backwards we identify $V = -C_1$. Several constraints may be applied to the size of the track gate. A minimum/maximum size for the gate can be set using the expected size of the object. Without realistic gate size constraints, the incoming detections may not fall within the association region. Figure 4 shows the sensor fusion results of the TWBLS. The individual sensor measurements for sensor 2 is also presented

for comparison with the fused estimates. Sensor 1 has a measurement error standard deviation of 8% and sensor 2 has a measurement error standard deviation of 15%. The advantage of sensor fusion is obvious from Fig. 4.



Error analysis and gating: Figure 4: Sensor data fusion for the TWBLS tracker. One of the published treatments of least squares projection algorithm postulated that the observed target location is the absolute target position at that time without any error.² According to this approach, the linear projection model is in error, not the observations. In this paper, both the linear projection model and the observations are assumed to be inexact since the targets may be maneuvering. The RMS error quantifying the difference between the observed response r_{ob} and the computed response r_c for N sample values is given by

$$RMS = \sqrt{\frac{1}{N} \sum_{i=1}^N (r_{ob} - r_c)^2} \quad (7)$$

The overall error of linear fit for the least squares projection is

$$EFIT = \sqrt{\frac{1}{N_{sample} - N_{par}} \sum_{i=1}^N (r_{ob} - r_c)^2}, \quad (8)$$

where $N_{par} = 2$ is the number of fitting coefficients. Covariance matrix $P = (F^T F)^{-1}$ is readily available from the least squares solution.

$$\begin{pmatrix} E_1 \\ E_2 \end{pmatrix} = EFIT \times \begin{pmatrix} \sqrt{P_{11}} \\ \sqrt{P_{22}} \end{pmatrix}, \quad (9)$$

here we identify $\Delta V^{az,el} = E_1$

Track-to-track correlation and fusion: The track fusion scheme for the TWBLS algorithm yielded sub-optimal results as shown in Figure 5. If fused appropriately, the fused state should be more accurate than the individual tracks that are combined for fusion. The track fusion scheme fuses two tracks with the more accurate sensor track shown for comparison with the fused track. The fused track performs better than the sensor track around 65% of the time. This is often the case with simplified track fusion techniques that do not take into account the dependence of the individual sensor tracks.^{7, 8, 9} Due to the same process noise, the two track estimation errors cannot be taken as independent. Therefore the information from the latest track estimate is not sufficient for optimal track fusion. Track fusion can often yield sub-optimal result even at the cost of vast computational load.

4. THE NOGA TRACKER

As presented in the case of the TWBLS algorithm, the track fusion node fails to obtain the “best” global state estimate given system constraints such as accuracy, computation load and bandwidth capacity. A demand for high accuracy in the global estimate leads to large computational load while simplified fusion methods yield poor track quality. In order to accommodate the possibly varying accuracy requirement and resource availability, an adaptive approach to track fusion is desirable. The NOGA tracker is presented in this section as an alternate approach to track fusion.

4.1. Auto-regressive model

The NOGA tracker employs a second-order auto-regressive model as the basic state estimator in conjunction with a novel uncertainty reduction approach. The NOGA tracking algorithm may be modified to incorporate other track estimator models.

$$y_\mu(k) = a_1^\mu y_\mu(k-1) + a_2^\mu y_\mu(k-2) + \dots + a_M^\mu y_\mu(k-M) \quad (10)$$

where μ denotes observation parameter such as $\mu = 1 = azimuth$ and $\mu = 2 = elevation$. For a second order Auto-Regressive (AR) model,

$$y_\mu(k-2) = a_1^\mu y_\mu(k-3) + a_2^\mu y_\mu(k-4) \quad (11)$$

$$y_\mu(k-1) = a_1^\mu y_\mu(k-2) + a_2^\mu y_\mu(k-3) \quad (12)$$

$$y_\mu(k) = a_1^\mu y_\mu(k-1) + a_2^\mu y_\mu(k-2). \quad (13)$$

The above formulations can be cast in matrix form to yield $Y_\mu = F^\mu a^\mu$ where $a^\mu = [a_1^\mu \ a_2^\mu]^T$ and

$$F^\mu = \begin{pmatrix} y_\mu(k-3) & y_\mu(k-4) \\ y_\mu(k-2) & y_\mu(k-3) \\ y_\mu(k-1) & y_\mu(k-2) \end{pmatrix}.$$

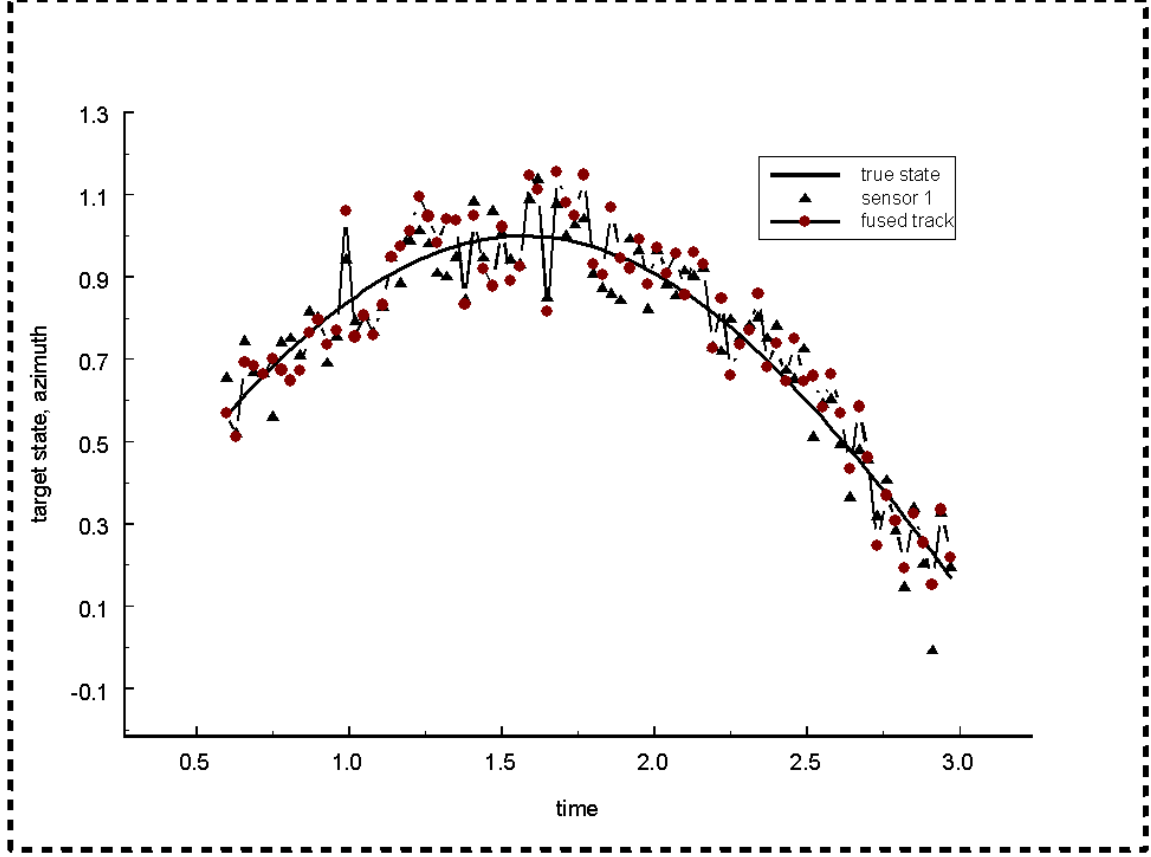


Figure 5: The NOGA tracker.

(14)

The idea is to give more weight to more recent data. Hence to second order

$$y_\mu(k) = a_1^\mu \Delta t_1 \frac{\exp^{-\Delta t_1}}{IFOV_\mu^2} y_\mu(k-1) + a_2^\mu \Delta t_2 \frac{\exp^{-\Delta t_2}}{IFOV_\mu^2} y_\mu(k-2). \quad (15)$$

As above, we can write this in matrix form as $Y_\mu = [y_\mu(k-2) \ y_\mu(k-1) \ y_\mu(k)]^T$ and

$$F_w(k) = \begin{pmatrix} \Delta t_3 \frac{\exp^{-\Delta t_3}}{IFOV_\mu^2} y_\mu(k-3) & \Delta t_4 \frac{\exp^{-\Delta t_4}}{IFOV_\mu^2} y_\mu(k-4) \\ \Delta t_2 \frac{\exp^{-\Delta t_2}}{IFOV_\mu^2} y_\mu(k-2) & \Delta t_3 \frac{\exp^{-\Delta t_3}}{IFOV_\mu^2} y_\mu(k-3) \\ \Delta t_1 \frac{\exp^{-\Delta t_1}}{IFOV_\mu^2} y_\mu(k-1) & \Delta t_2 \frac{\exp^{-\Delta t_2}}{IFOV_\mu^2} y_\mu(k-2) \end{pmatrix}. \quad (16)$$

To solve for the fitting parameters, the pseudo-inverse technique is used as $a^\mu = (F_w^T F_w)^{-1} F_w Y_\mu$. The track estimation errors are computed according to the formulation presented in the next subsection.

4.2. Uncertainty reduction

Accuracy, robustness, and timely prediction are the key merits in track estimation. Predictability is challenged by inherent uncertainties at the theoretical and experimental levels. Theoretical uncertainties arise from unavoidable simplifications carried out in the modeling process and experimental uncertainties occur due to noise, imperfect conditions and human errors. A general uncertainty analysis (UA) framework that allows for the consistent determination and sharpening of confidence limits for the outputs of a mathematical model of a physical system, by combining the model predictions with experimental evidence is presented here.^{3, 10, 11} This is a time-independent model. Bold lowercase letters denote vectors and bold uppercase letters denote matrices, and \sim denotes transpose. The model parameters and inputs are contained in vector \mathbf{a} , the calculated responses are collected in vector \mathbf{q} , and the measured or experimental response is \mathbf{r} . The nominal uncertainties in the parameters are given by the covariance matrix $\mathbf{C}_a = \langle \Delta \mathbf{a} \Delta \tilde{\mathbf{a}} \rangle$. Here $\Delta \mathbf{a}$ denotes the vector of standard deviations and the brackets denote expectation (integration over a joint probability density function). In this approach, no specific forms of the PDF is required. The first two moments, the mean value and the covariance can be calculated directly from empirical observation without using any specific PDF. The sensitivity of the calculated response (q_n) to parameter (a_i) are computed at the nominal parameter values as

$$\mathbf{S}_{ni} = \frac{\partial q_n}{\partial a_i} \Big|_{\mathbf{a}}. \quad (17)$$

Sensitivities can be calculated using adjoint operator formulation or automated differentiation techniques. If higher order sensitivities are needed, they can be calculated from first order matrices. The sensitivity matrix \mathbf{S} allows one to calculate the nominal covariance matrix of the calculated responses as $\mathbf{C}_q = \langle \Delta \mathbf{q} \Delta \tilde{\mathbf{q}} \rangle = \mathbf{S} \mathbf{C}_a \tilde{\mathbf{S}}$. Even if the nominal covariance matrix of the system parameters is diagonal, the covariance matrix of the computed model responses is a full. Next the best estimates for the parameters ($\hat{\mathbf{a}}$) and the responses ($\hat{\mathbf{r}}$) are calculated. To first order:

$$\hat{\mathbf{r}} - \mathbf{r} = \mathbf{q} - \mathbf{r} + \mathbf{S}(\hat{\mathbf{a}} - \mathbf{a}). \quad (18)$$

New variables are defined: $\mathbf{x} = \hat{\mathbf{a}} - \mathbf{a}$, $\mathbf{y} = \hat{\mathbf{r}} - \mathbf{r}$, and the discrepancy between calculated and measured responses $\mathbf{e} = \mathbf{q} - \mathbf{r}$. Using the new variables, the local functional relationship between the system parameters and responses becomes $\mathbf{y} = \mathbf{S}\mathbf{x} + \mathbf{e}$. To obtain the best estimate, the computational and the experimental results must be consistently combined. This is achieved by optimizing a Bayesian loss function that simultaneously minimizes the difference between the best estimate responses and the measured responses, and the best estimate and the calculated parameters as

$$Q = \left(\tilde{\mathbf{y}} | \tilde{\mathbf{x}} | \dots \right) \begin{pmatrix} \mathbf{C}_r & \mathbf{C}_p & \dots \\ \tilde{\mathbf{C}}_p & \mathbf{C}_a & \dots \\ \dots & \dots & \dots \end{pmatrix}^{-1} \begin{pmatrix} \mathbf{y} \\ \mathbf{x} \\ \dots \end{pmatrix}. \quad (19)$$

\mathbf{C}_r represents the covariance matrix of the measured responses, \mathbf{C}_p represents the covariance matrix due to the response-parameters correlations and the three dot patterns denote additional covariance and cross-covariance that may be included. The loss function must be constrained in terms of the functional relationship between the parameters and the responses. This relationship was locally approximated to first order only. If the responses are strongly nonlinear, an iterative procedure must be implemented. An augmented Lagrangian is defined as $L = Q + \lambda^T [Sx - y - e]$. The necessary conditions for a locally optimal solution are obtained by requiring that the partial derivatives of the augmented Lagrangian with respect to \mathbf{x} and \mathbf{y} be zero. These equations are solved in conjunction with the constraints satisfaction to obtain the optimal values of \mathbf{x} and \mathbf{y} , which yield the best estimates for both the parameters and the responses. The best estimates of the covariance matrices have reduced uncertainties. After lengthy algebra,

$$\hat{\mathbf{a}} = \mathbf{a} + \left(\tilde{\mathbf{C}}_p - \mathbf{C}_a \tilde{\mathbf{S}} \right) \lambda, \quad \lambda = \left(\mathbf{C}_r - \mathbf{S} \tilde{\mathbf{C}}_p - \mathbf{C}_p \tilde{\mathbf{S}} + \mathbf{S} \mathbf{C}_a \tilde{\mathbf{S}} \right)^{-1} \mathbf{e}, \quad \hat{\mathbf{r}} = \mathbf{r} + \left(\tilde{\mathbf{C}}_r - \mathbf{C}_p \tilde{\mathbf{S}} \right) \lambda. \quad (20)$$

Note that the above best estimate \hat{r} differs from the model-predicted response that would be computed using the best estimate values for the system parameters as $\hat{\mathbf{q}} = \mathbf{q}(\hat{\mathbf{a}})$. The covariance matrix corresponding to the best estimates of the system parameters is given by

$$\mathbf{C}_{\hat{\mathbf{a}}} = \mathbf{C}_{\mathbf{a}} - \left(\tilde{\mathbf{C}}_{\mathbf{p}} - \mathbf{C}_{\mathbf{a}}\tilde{\mathbf{S}} \right) \left(\mathbf{C}_{\mathbf{r}} - \mathbf{S}\tilde{\mathbf{C}}_{\mathbf{p}} - \mathbf{C}_{\mathbf{p}}\tilde{\mathbf{S}} + \mathbf{S}\mathbf{C}_{\mathbf{a}}\tilde{\mathbf{S}} \right)^{-1} \left(\mathbf{C}_{\mathbf{p}} - \mathbf{S}\mathbf{C}_{\mathbf{a}} \right). \quad (21)$$

The covariance matrix corresponding to the best estimates of the responses is

$$\mathbf{C}_{\hat{\mathbf{r}}} = \mathbf{C}_{\mathbf{r}} - \left(\mathbf{C}_{\mathbf{r}} - \mathbf{C}_{\mathbf{p}}\tilde{\mathbf{S}} \right) \left(\mathbf{C}_{\mathbf{r}} - \mathbf{S}\tilde{\mathbf{C}}_{\mathbf{p}} - \mathbf{C}_{\mathbf{p}}\tilde{\mathbf{S}} + \mathbf{S}\mathbf{C}_{\mathbf{a}}\tilde{\mathbf{S}} \right)^{-1} \left(\mathbf{C}_{\mathbf{r}} - \mathbf{S}\tilde{\mathbf{C}}_{\mathbf{p}} \right). \quad (22)$$

The covariance matrix associated with the model responses recalculated using the best estimates of the system parameters is, to first order, simply $\mathbf{C}_{\hat{\mathbf{q}}} = \mathbf{S}_{\hat{\mathbf{a}}}\mathbf{C}_{\hat{\mathbf{a}}}\tilde{\mathbf{S}}_{\hat{\mathbf{a}}}$, where the sensitivities must be recalculated at the new parameter values $\hat{\mathbf{a}}$. Finally it is noted that the best estimate for the covariance matrix associated with the response-parameter correlations is given by

$$\mathbf{C}_{\hat{\mathbf{p}}} = \mathbf{C}_{\mathbf{p}} - \left(\mathbf{C}_{\mathbf{r}} - \mathbf{C}_{\mathbf{p}}\tilde{\mathbf{S}} \right) \left(\mathbf{C}_{\mathbf{r}} - \mathbf{S}\tilde{\mathbf{C}}_{\mathbf{p}} - \mathbf{C}_{\mathbf{p}}\tilde{\mathbf{S}} + \mathbf{S}\mathbf{C}_{\mathbf{a}}\tilde{\mathbf{S}} \right)^{-1} \left(\mathbf{C}_{\mathbf{p}} - \mathbf{S}\mathbf{C}_{\mathbf{a}} \right). \quad (23)$$

A reduction in the uncertainties of the system parameters means that in general each diagonal term of $\mathbf{C}_{\hat{\mathbf{a}}}$ is less than or equal to the corresponding diagonal term of $\mathbf{C}_{\mathbf{a}}$.³ The tracking performance of the NOGA tracker is compared with that of the TWBLS in Fig. 6. As can be seen the NOGA tracker shows superior performance compared to TWBLS.

5. SUMMARY

Two algorithms are presented in this paper for small target detection applications as alternatives to the standard Kalman/extended Kalman filter techniques. The TWBLS tracker can perform well in an asynchronous multi-sensor environment. The main advantage of the NOGA tracker is the ability to react to the changes in the sensor environment to avoid useless or even penalizing fusion. Further research is ongoing for application of the NOGA tracker in a multi-sensor multi-target environment.

REFERENCES

- [1] Y. Bar-Shalom, *Estimation with Application to Tracking and Navigation*, John Wiley and Sons Inc., New York, 2001.
- [2] J. N. Sanders-Reed, "A software architecture for real-time target detection, tracking, and signature extraction," *Proceeding of the SPIE*, **2468**, 1-12, 1995.
- [3] J. Barhen, D. G. Cacuci, J. J. Wagschal, M. A. Bjerke, and C. B. Mullins, "Uncertainty analysis of time-dependent nonlinear systems," *Nuclear Science and Engineering*, **81**, 23-44, 1982.
- [4] R. A. Singer and J. Kanyuck, "Computer control of multiple site track correlation," *Automatica*, **7**, 455-463, 1971.
- [5] Y. Bar-Shalom and X. R. Li, *Multitarget-Multisensor Tracking: Principles and Techniques*, John Wiley and Sons Inc., New York, 1995.

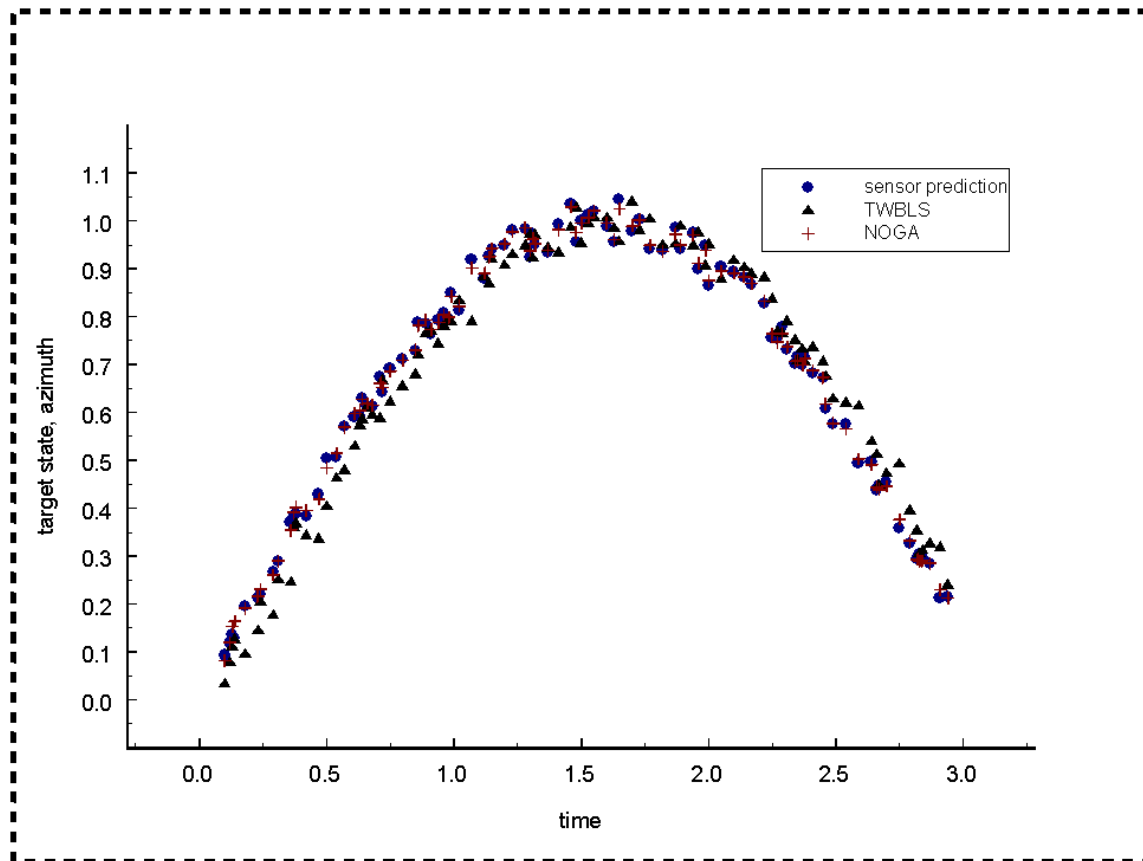


Figure 6: The NOGA tracker.

- [6] J. A. Roecker and C. D. McGillem, "Comparison of two-sensor tracking methods based on state vector fusion and measurement fusion," *IEEE Transactions on Aerospace and Electronic Systems*, **24**, 447-449, 1988.
- [7] K. C. Chang, R. K. Shaha, and Y. Bar-Shalom, "On Optimal track-to-track fusion," *IEEE Transactions on Aerospace and Electronics Systems*, **33**, 1271-1276, 1997.
- [8] Y. Bar-Shalom, "On the track-to-track correlation problem," *IEEE Transactions on Automatic Control*, **26**, 571-572, 1981.
- [9] Y. Bar-Shalom, "The effect of common process noise on the two-sensor fused-track covariance," *IEEE Transactions on Aerospace and Electronic Systems*, **22**, 803-805, 1986.
- [10] J. Barhen and D.G. Cacuci, "An efficient procedure to evaluate second-order sensitivities for nonlinear problems with nonlinear responses," *Transactions of the American Nuclear Society*, **35**, 266-267, 1980.
- [11] J. Barhen, J. J. Wagschal, and Y. Yeivin, "Lagrange multipliers in data adjustment with response-parameter correlations," *Transactions of the American Nuclear Society*, **35**, 246-247, 1980.